Available online at www.sciencedirect.com
ScienceDirect
International Journal of Thermal Sciences 47 (2008) 659–667
International Journal of Thermal Sciences
www.elsevier.com/locate/ijts

Thermal performance of closed two-phase thermosyphon using nanofluids

Sameer Khandekar [a,*], Yogesh M. Joshi [b], Balkrishna Mehta [a]

[a] *Department of Mechanical Engineering, Indian Institute of Technology Kanpur, Kanpur 208016, India*
[b] *Department of Chemical Engineering, Indian Institute of Technology Kanpur, Kanpur 208016, India*

Received 15 February 2007; received in revised form 4 June 2007; accepted 6 June 2007

Available online 16 July 2007

Abstract

Nanofluids, stabilized suspensions of nanoparticles typically <100 nm in conventional fluids, are evolving as potential enhanced heat transfer fluids due to their improved thermal conductivity, increase in single phase heat transfer coefficient and significant increase in critical boiling heat flux. In the present paper, we investigate the overall thermal resistance of closed two-phase thermosyphon using pure water and various water based nanofluids (of Al_2O_3, CuO and laponite clay) as working fluids. We observe that all these nanofluids show inferior thermal performance than pure water. Furthermore, we observe that the wettability of all nanofluids on copper substrate, having the same average roughness as that of the thermosyphon container pipe, is better than that of pure water. A scaling analysis is presented which shows that the increase in wettability and entrapment of nanoparticles in the grooves of the surface roughness cause decrease in evaporator side Peclet number that finally leads to poor thermal performance.

Keywords: Nanofluids; Pool boiling; Two-phase closed thermosyphon and Wettability

1. Introduction

For the past many years, two-phase passive heat transfer devices like heat pipes and thermosyphons have played an important role in a variety of engineering heat transfer systems, ranging from electronics thermal management to heat exchangers and reboilers. In this context, the present scenario of high thermal loading coupled with high flux levels demands exploration of new heat transfer augmentation mechanisms besides the conventional techniques. 'Nanofluids' are fast emerging as alternatives to conventional heat transfer fluids [1]. Although recent studies have shown some conflicting trends with regards to their thermo-hydrodynamic behavior (refer to Section 2), there are enough indications that exploratory research is indeed required to bench mark the scope and applicability of these fluids in engineering systems. With this aim, the present work aims to study the effects of nanofluids on thermal performance of a closed two-phase gravity assisted thermosyphon.

The term 'Nanofluids' is used to indicate a newly introduced special class of heat transfer fluids that contain nanoparticles (<∼100 nm) of metallic/non-metallic substances uniformly and stably suspended in a conventional heat transfer liquid [1]. Recent studies have indicated that by adding nanoparticles to conventional fluids can alter the thermophysical and transport properties of the base fluid (refer to Section 2). Thus, the introduction of nanofluids has given an impetus to the idea of developing tailor made fluids best suited for a given heat transfer application. Therefore, in principle, a working fluid with 'better' thermophysical properties can be engineered/tailor-made to potentially enhance the device performance. Which of the thermo-physical properties need alteration by the addition of nanoparticles? This question has to be addressed in light of the mechanisms governing the device performance.

In a gravity-assisted thermosyphon, the basic mechanisms of heat transfer are nucleate pool boiling (under closed confined conditions) in evaporator and filmwise condensation in the condenser sections respectively. In both these phase-change mechanisms, thermophysical properties of the working fluid along with characteristic features of the solid substrate play an important role in deciding the heat transfer rates. In this pa-

* Corresponding author. Tel.: +91 512 2597038; fax: +91 512 2597408.
E-mail address: samkhan@iitk.ac.in (Sameer Khandekar).

1290-0729/$ – see front matter
doi:10.1016/j.ijthermalsci.2007.06.005

Nomenclature

A	area of cross-section	m^2
Bo	Bond number ($d[g(\rho_l - \rho_v)/\sigma]^{1/2}$)	
C_p	specific heat at constant pressure	J/kg K
d	diameter of thermosyphon	m
g	acceleration due to gravity	m/s^2
h	heat transfer coefficient	W/m^2 K
h_{fg}	latent heat of vaporization	J/kg
$\widehat{Ku}$	Kutateladze number	
k	thermal conductivity	W/m K
L	length	m
Nu	Nusselt number ($h \cdot L/k$)	
n'_a	active nucleation site density	m^{-2}
$\dot{Q}$	heat throughput rate	W
q''	heat flux	W/m^2
R	radius	m
R_a	average surface roughness	m
R_q	rms surface roughness	m
R_z	peak-to-valley surface roughness	m
Re	Reynolds number ($\rho U L/\mu$)	
R_{th}	thermal resistance	K/W or °C/W
Pr	Prandtl number ($\mu C_p/k$)	
T	temperature	°C or K
U	velocity	m/s
V	volume	m^3

Greek symbols

μ	dynamic viscosity	N s/m^2
γ	cavity half angle	rad
ρ	mass density	kg/m^3
σ	surface tension	N/m
θ	contact angle	rad
v	specific volume	m^3/kg

Subscripts

a	adiabatic section
axi	axial
b	bubble
c	condenser section
crit	critical
e	evaporator section
f	fluid
l	liquid
o	outer, outlet
rad	radial
sat	saturation
v	vapor
w	wall

Abbreviations

BL	Boiling Limitation
CHF	Critical Heat Flux
CCFL	Counter Current Flooding Limitation
FR	Filling Ratio of the working fluid (V_l/V_e) at room temperature

per we investigate thermal performance of various nanofluids and benchmark the same with respect to pure water for closed two-phase thermosyphon. We observe that the thermal performance of nanofluids is significantly influenced by alteration in the fluid/solid interface due to presence of nanoparticles.

2. Literature review

Heat transfer fluids containing suspensions of nanoparticles were first reported by Choi in 1995 [1]. Subsequent studies by the same group reported that a small amount (less than 1% by volume fraction) of copper nanoparticles in ethylene glycol can increase the inherently poor thermal conductivity by 40%. They also suggested some possible mechanisms of thermal transport that leads to such enhancement [2–5]. Similar thermal conductivity enhancement for a variety of nanoparticles/base fluid systems has been reported by other groups also [6–9]. Significantly, Das et al. [10] showed that effective thermal conductivity of nanofluids increases with increase in temperature. This finding makes nanofluids even more attractive as a cooling fluid for devices with high energy density. Past few years have seen many researches involved in measurement of single phase convective heat transfer rates using nanofluids with many groups reporting increase in forced convection rates [11–14]. On the other hand, opposite trends have also been reported in the literature [15,16].

With regards to pool boiling heat transfer, Witharana (as reported in [11]) investigated the heat transfer coefficients of Au/water, SiO_2/water, and SiO_2/ethylene glycol nanofluids under pool boiling conditions. Results of Au/water nanofluids showed an increase of heat transfer rates compared to that of pure water while the SiO_2/water and SiO_2/ethylene glycol nanofluids showed a reverse trend. Li et al. [17] conducted experiments to study the sub-cooled pool boiling characteristics of SiO_2/water nanofluid on Pt-wires and found deterioration in heat transfer. Das et al. [18] carried out an experimental study of pool boiling characteristics of Al_2O_3 nanofluids under atmospheric conditions on a tube with diameter in 20 mm. They found that the inclusion of nanoparticles degraded the boiling performance by increasing the wall superheat for a given heat flux. They speculated that the deterioration in boiling performance was not due to change in fluid property but due to the change in surface property because of entrapment of nanoparticles in the surface cavities (grooves).

You et al. [19] have also reported the deterioration in boiling heat transfer coefficient but found drastic enhancement in

critical heat flux (CHF) for Al_2O_3 nanofluids. They performed visualization study and found that the average size of departing bubble increases but the frequency of departing bubble decreases. Bang and Chang [20] studied the boiling heat transfer using Al_2O_3–water nanofluids on a horizontal smooth surface. They showed that nanofluids have poor heat transfer coefficient as compared to pure water in natural convection as well as in nucleate boiling. They also reported enhancement in CHF in both, horizontal and vertical pool of liquid. However, on the contrary, Tu et al. [21] found significant enhancement in pool boiling heat transfer for Al_2O_3 nanofluid. Vassallo et al. [22] compared the heat transfer performance of pure water, silica nano-solutions and silica micro-solutions under atmospheric pressure with a 0.4 mm NiCr wire submerged in each solution. Their data show a marked increase in critical heat flux for both micro and nano-solutions compared to that of water, but no appreciable differences in heat transfer for heat powers less than CHF. They speculated that roughness of the solid substrate might be responsible for the observed behavior. Milanova and Kumar [23] showed that property of silica nano-suspensions changes with ionic concentration, particle size and pH of the nanofluid. They also showed that the surface structure of the deposition affects the thermal properties of the liquid. Kim et al. [24,25] argued that under boiling conditions there is a buildup of a porous layer of nanoparticles on the heated surface, which significantly improves the surface wettability of the surface. This can plausibly explain the CHF enhancement in nanofluids. On a different note, Sefiane [26] argued that nanoparticles promote the pinning of the contact line of the meniscus and sessile drops due to the presence of structural disjoining pressure that can possibly explain the increase in CHF.

Thus, the recent literature, although still sparse, suggests the following emerging key features of the nanofluids:

(i) Enhanced thermal conductivities as compared to conventional solid–liquid suspensions.
(ii) Strongly non-linear temperature dependent effective thermal conductivity.
(iii) An increase in single-phase heat transfer coefficient while a decrease in pool boiling heat transfer coefficient.
(iv) An increase in CHF under pool boiling conditions.

The observed behavior of nanofluids is in many ways anomalous with respect to the predictions of existing macroscopic theory. In addition, as has been noted above, since this subject of nanofluids is still emerging and overall understanding is in its infancy, there are contradictory trends reported in the literature.

3. Design of experiment

The main objective of the present work is to study the thermal performance of a closed two-phase thermosyphon with different water based nanofluids, to check the potential enhancement, if any, as compared to standard working fluid i.e. degassed de-ionized water. With this aim, an experimental setup of gravity-assisted thermosyphon based on maximum heat flux was designed, fabricated and tested. Gravity assisted thermosyphon is known to have limitations like dry-out limitation, Counter Current Flow Limitation (CCFL) or flooding, boiling limitation, etc. Dryout limitation is usually not important unless the filling ratio (FR) is less than 40%. If FR is above this limit, dry out phenomenon is not observed and other mechanisms like CCFL/flooding or Boiling Limitation (BL) [27] limit the maximum heat flux. In the present experiments, since the FR was always 100%, dry-out limitation was not a relevant consideration.

The Counter Current Flow Limitation (CCFL) is one of the most important and common limitations found in closed two-phase thermosyphons. According to the classical theory proposed by Wallis and Kutateladze [27–29], and its modifications by Tein and Chung [30] and Faghri et al. and other groups [27], the generally accepted correlation for CCFL is given by:

$$\widehat{Ku}_{\mathrm{CCFL}} = \frac{(Q_{\max}/A_{\mathrm{axi}})}{h_{fg}\rho_v^{0.5}[g\sigma(\rho_l-\rho_v)]^{1/4}} \tag{1}$$

where

$$\widehat{Ku}_{\mathrm{CCFL}} = \tilde{K}/\left[1+(\rho_v/\rho_l)^{1/4}\right]^2 \tag{2}$$

$$\tilde{K} = \left(\frac{\rho_l}{\rho_v}\right)^{0.14}\cdot \tanh^2 Bo^{1/4} \tag{3}$$

and

$$Bo = d\left[g(\rho_l-\rho_v)/\sigma\right]^{1/2} \tag{4}$$

The Boiling Limitation (BL) is observed in thermosyphons having large liquid fill ratio and high radial heat fluxes in the evaporator section. Under this limitation, at the critical heat flux, vapor bubbles coalesce near the pipe wall that prohibits the contact of working liquid to wall surface resulting in rapid increase in evaporator wall temperature. Golobič and Gašperšič [31] have complied many CCFL and boiling limitation correlations available for closed two-phase thermosyphons. For Boiling Limitation, we make use of the correlation suggested by Imura et al. [32] which provides a good estimate given by:

$$\widehat{Ku}_{\mathrm{BL}} = \frac{(Q_{\max}/A_{\mathrm{rad}})}{h_{fg}\cdot\rho_v^{0.5}[g\sigma(\rho_l-\rho_v)]^{1/4}} \tag{5}$$

where

$$\widehat{Ku}_{\mathrm{BL}} = 0.16\left[1-\exp\left\{(-d/L_e)(\rho_l/\rho_v)^{0.13}\right\}\right] \tag{6}$$

Comparing Eqs. (1) and (5) along with Eqs. (2) and (6), we note the following:

(a) Both Eqs. (1) and (5) are identical except the fact that the area of cross section of the thermosyphon ($A_{\mathrm{axi}} = \pi d^2/4$) is applicable in Eq. (1), while the radial evaporator area ($A_{\mathrm{rad}} = \pi d L_e$) is in the latter. The denominator in both the equations is a direct manifestation of interface instability analysis coupled with dimensional analysis developed simultaneously by Kutateladze [33] and Taylor (as given in [27]).
(b) It is seen from Eq. (2) that the parameter $\tilde{K}$ takes into account the effect of the curvature of the container in terms of the non-dimensional diameter, Bond number. There is no explicit dependency on the (L_e/d) in Eq. (2) as can be seen

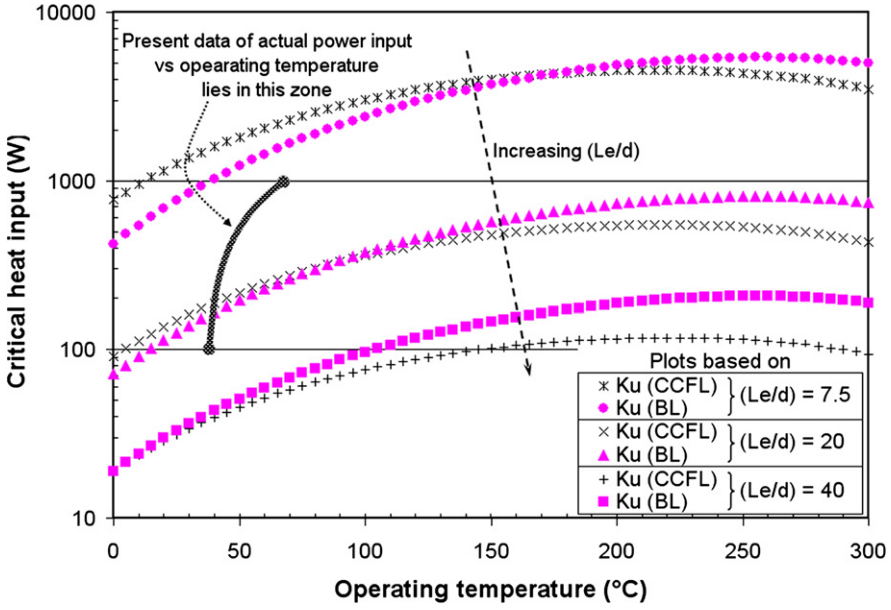

Fig. 1. Effect of aspect ratio (L_e/d) on the Kutateladze number (Ku) for different heat throughput limitation.

in Eq. (6) but previous studies show that when the ratio of evaporator length to its diameter, L_e/d, is greater than 60, CCFL/flooding phenomena prevail. When $L_e/d \leqslant 3$–5, pool boiling characteristics have significant influence in limiting the heat throughput. In the intermediate range of L_e/d, it is difficult to explicitly differentiate between the above two limitations.

The above discussed aspects of the limitations can be seen clearly in Fig. 1, where the maximum heat throughput, which is possible, based on CCFL condition (Eqs. (1), (2)) and BL condition (Eqs. (5), (6)), is plotted. It is clearly observed that in the operating temperature range of 30–70 °C, BL predominates for low aspect ratios (L_e/d) while CCFL dominates at higher aspect ratios. Moreover, we can clearly distinguish the difference between BL and CCFL at lower aspect ratios. As aspect ratio increases, respective critical heat fluxes tend to overlap with each other, thereby making it difficult to distinguish which phenomenon is responsible for the eventual burnout of evaporator wall, CCFL or BL.

In the present study, we chose an aspect ratio of 7.5 (as indicated in Fig. 1) with $L_e = 120$ mm and $d = 16$ mm so as to render the device exclusively limited under boiling limitation, at least from theoretical considerations as discussed above. This design was chosen in the wake of recent indicative studies, as mentioned earlier, where nanofluids show a higher CHF under pool boiling conditions. The set-up allowed a controllable heat input from 0–1200 W. For a given experimental run, condenser-cooling water was maintained at a specific level, and the heat input to the evaporator was slowly increased till the desired steady state operating temperature was obtained. The adiabatic operating temperatures ranged from 40 to 65 °C. Externally controlled conditions were kept identical for baseline experiments with pure water and those with nanofluids. Various actual conditions under which the present experiments were conducted are also highlighted in Fig. 1 by the thick solid line. Thus, the thermosyphon is always operated under 'normal' operating conditions and its performance in terms of net thermal resistance could be ascertained, as reported in the present work.[1]

4. Description of setup and procedure

The details of the set-up, along with relevant dimensions, are shown in Fig. 2. A pressure transducer fitted to the thermosyphon monitored proper initial vacuum level and subsequent saturation pressure profiles. Heat was supplied to the evaporator by a copper heating block with dimension of 120 mm × 50 mm × 50 mm that had a center bore to accommodate the thermosyphon container with a tight press fit (thermally conducting heat sink compound was used prior to fitment). Four mica insulated surface heaters (116 mm × 48 mm) were mounted on the outer surface of the block with the help of a stainless steel backing plate.

Finned tube condenser was made for the heat removal from the thermosyphon. Forty square copper fins of 70 mm × 70 mm × 1 mm size were brazed at a pitch of 6.5 mm to each other. The inlet and outlet of the shell side were designed in such a manner that cross-flow conditions existed over the condenser fins. A constant temperature bath (Haake® cryostat, model DC-10-K-20) was used to circulate the cooling water maintained at 30 °C to the condenser. Eight thermocouples (sheath protected, K-type) were used to measure the temperature at important axial locations on the thermosyphon tube as shown in Fig. 2. PC based data acquisition was carried out by

[1] The determination of limiting behavior under critical boiling heat flux conditions necessitated upgraded control of the condenser cooling conditions so as to maintain isothermal conditions for cooling water; due to unavailability of the upgraded control, CHF behavior of nanofluids in thermosyphons is not reported here.

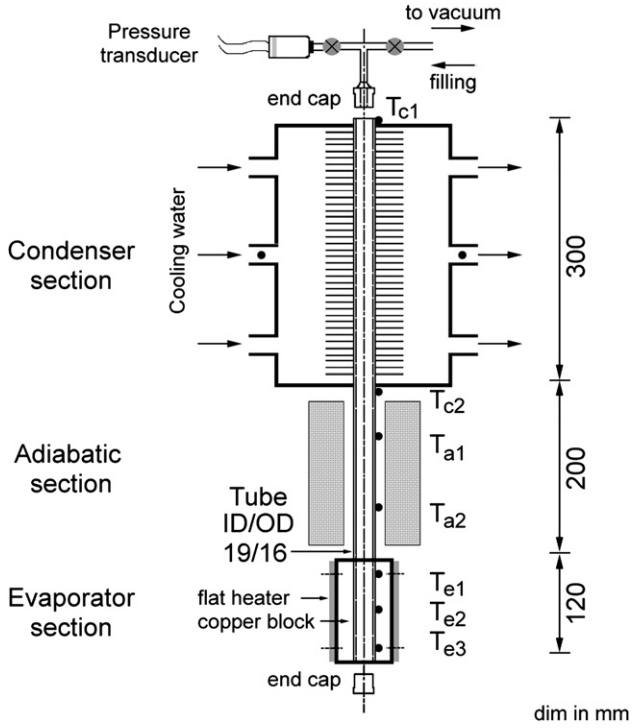

Fig. 2. Schematic of the experimental setup.

a high precision data acquisition system (NI-PCI-4351 by National Instruments®).

Before proceeding to test nanofluids, baseline experiments were conducted with degassed and deionized water. Once the quality and repeatability of the baseline data was established, then three water based nanofluids (1% of nanoparticle by weight in all the cases), namely CuO (8.6 to 13.5 nm), Al_2O_3 (40–47 nm) and laponite JS clay (discs of diameter 25 nm and thickness 1 nm), were used as the working fluids. Nanoparticles were procured from established commercial venders.[2] Laponite has a chemical formula $Na^{+0.7}[(Si_8Mg_{5.5}Li_{0.3})O_{20}(OH)_4]^{-0.7}$ and is a colloidal synthetic layered silicate; the sol-forming variant of laponite has been used in the present study containing Tetrasodium Phosphate (quantity w/w is proprietary information) which facilitates sol formation. The sizes of alumina and CuO nanoparticles were obtained by carrying out XRD/TEM on the respective samples, while that of laponite is obtained from the supplier.

After dispersing the respective nanoparticles in the base fluid, these were subjected to ultrasonication for about two hours. In the case of alumina and laponite, stable suspensions were obtained and no precipitation/settlement of particles was seen for several weeks. However, CuO based nanofluid was difficult to stabilize as compared to the other two fluids in the stationary state, requiring much severe ultrasonication. While long-term stability of these nanofluids needs to be addressed separately, in this study we did not add any special reagent or surfactant. Furthermore, importantly, given that the thermosyphon testing conditions involve vigorous boiling, we believe that any aggregates are not likely to be formed in the experimental timescales.

Thorough cleaning of the device is vital for the success of the experiment and reliability/repeatability of the data. The changeover from one nanofluid to the other must be preceded by a reliable cleaning protocol for ensuring that there are no remaining remnants of the earlier sample inside the device. This was achieved by three-cycle operation of cleaning/rinsing with deionized water, acetone and ethanol and vacuum drying. This was followed by another cycle in which the device was placed inside an ultra-sonicator with continuous rinsing with water. Finally, the tube was cured under vacuum ($<10^{-3}$ mbar) for extended period of time. This procedure was followed for every changeover of the working fluid. In between every changeover, the device was first tested with deionized and degassed water to repeatedly generate the baseline data for thermal resistance.

5. Results and discussion

Fig. 3 shows the comparative results of thermal resistance of thermosyphon with pure water and various nanofluids. We have defined the thermal resistance as:

$$R_{\text{th}} = (T_e - T_c)/\dot{Q} \tag{7}$$

where, T_e and T_c are average values of the respective locally placed thermocouples (refer to Fig. 2). Interestingly, all the nanofluids, show inferior thermosyphon performance of varying degree compared to that of water. We believe that, in order to understand the effect of incorporation of nanoparticles in the base fluids, on the thermal performance of a thermosyphon, we need to focus our attention on following two aspects. First being effect of nanoparticles on pool boiling characteristics in the evaporator, and other is the effect of nanoparticles on condensation heat transfer characteristics. The condenser section needs scrutiny only under the hypothetical premise that nanoparticles are transported upwards in that zone by the inertia of the vapor. There is no conclusive evidence to support this hypothesis, but the fact that, even micrometer sized pollutant particulates do not settle down for extended periods of time in the atmosphere indicates that this possibility cannot be ruled out. However, this issue needs to be addressed separately. In this paper we will concentrate on the effect of nanoparticles on pool boiling characteristics in the evaporator section.

Literature suggests that there is an enhancement in single-phase heat transfer coefficient with nanofluids. Under laminar flow conditions, heat transfer coefficient is a linear function of fluid thermal conductivity. Under turbulent flow conditions, classical Dittus–Boelter correlation suggests that:

$$h_{\text{conv}} \propto [C_p/\mu_l]^{2/5}[k_l]^{3/5} \tag{8}$$

Thus, even for a turbulent flow field, the convective heat transfer increases with thermal conductivity of the base fluid. Therefore, in case of single-phase convective heat transport, the increase in thermal conductivity of the base fluid, due to addition of nanoparticles, can possibly explain the corresponding increase

[2] www.sigmaaldrich.com and Southern Clay Products, Inc., www.laponite.com.

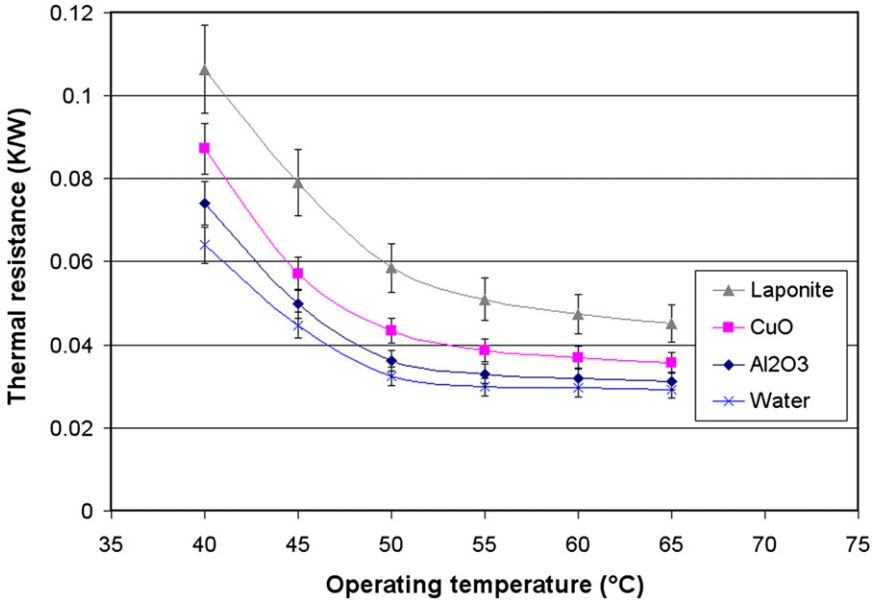

Fig. 3. Thermal resistance of the thermosyphon with different nanofluids as compared to pure water.

in the heat transfer coefficient. This requires further investigation.

Under pool boiling conditions, as reported earlier (refer Section 2), a reduction in heat transfer coefficient is generally observed, which also is the case of present experimental results on closed two-phase thermosyphon. Looking at this trend, in the wake of the contrasting increase in single-phase heat transfer coefficient, the classical Rohsenow/Froster–Zuber correlations for pool boiling [34], which are based on single-phase convection analogy, suggests possible reasoning behind the observed phenomenon. During nucleate pool boiling, the single-phase convective transport gets patently affected by many complimentary effects such as bubble departure diameter, frequency of bubble departure, nucleation site density and the average rise velocity of individual bubbles. There is a possibility that the addition of nanoparticles might be adversely affecting the impact of these parameters on the pool boiling heat transfer. The adverse effects seem to be stronger than the complementary increase in single-phase heat transfer coefficient brought solely by the increased thermal conductivity of the nanofluid. The fact that an unequivocal degradation of thermal performance occurs under nucleate pool boiling regime, indicates the need to study the interplay between the suspended nanoparticles with the heater wall surface.[3]

Practically all models describing nucleate boiling heat transfer suggest a power law dependence of nucleate boiling heat flux on the nucleation site density and the wall superheat given by [34]:

$$q'' = (n'_a)^x (T_w - T_{\text{sat}})^y \tag{9}$$

Various classical models suggest different values of exponents x and y. In general, for most of the models, x varies between 0.3 and 0.5 while y varies between 1.0 and 1.8 [34,35]. In case of nanofluids, the active nucleation site density n'_a can get affected by two mechanisms: (i) physical adhesion, blockage, gradual filling up of active nucleation sites with nanoparticles thereby increasing the cavity (groove) half angle γ and/or reducing the cavity mouth radius (see Fig. 4), (ii) a change in contact angle/wetting characteristics of the base fluid on the heater surface due to the addition of nanoparticles.

Referring to Fig. 4(a), if R denotes the cavity radius, and the minimum interface radius during embryo growth is denoted by $r_{\min}$, the condition for the cavity to be active can be stated as:

$$T_l - T_{\text{sat}} > \frac{2 \cdot \sigma \cdot T_{\text{sat}} \cdot \nu_{lv}}{h_{lv} \cdot r_{\min}} \tag{10}$$

For the situations where the contact angle θ is large and $R/r \leqslant 1$, $r_{\min}$ can be approximated by R and then Eq. (10) can be written as:

$$T_l - T_{\text{sat}} > \frac{2 \cdot \sigma \cdot T_{\text{sat}} \cdot \nu_{lv}}{h_{lv} \cdot R} \tag{11}$$

This equation clearly suggests that as the cavity mouth radius, R decreases (which may be due to physical adhesion, blockage etc., as suggested above), then a higher superheat is required to activate a given site.

To investigate this aspect further, the internal surface roughness of the thermosyphon copper pipe before the experiments was measured (by a laser profilometer) and found to be $R_a = 0.24$ μm, $R_z = 1.83$ μm and $R_q = 0.31$ μm. Since it was not possible to destructively break open the thermosyphon container after every test (to study the effect of boiling nanofluids on the surface roughness), a separate flat copper substrate

[3] The bulk thermal conductivity of metal oxide nanoparticles (CuO = 32.6 W/m-K and Al_2O_3 = 40 W/m-K) is an order of magnitude higher than that of water whereas for laponite the same is quite low (bulk laponite = 0.15 W/m-K). While pool boiling heat transfer depends on the interaction and interplay of many parameters simultaneously (thermal conductivity of the fluid being one of them), the trend in the thermal performance of the thermosyphon, although it follows the trend in the bulk thermal conductivity of the used nanoparticles, cannot be fully attributed to this sole effect.

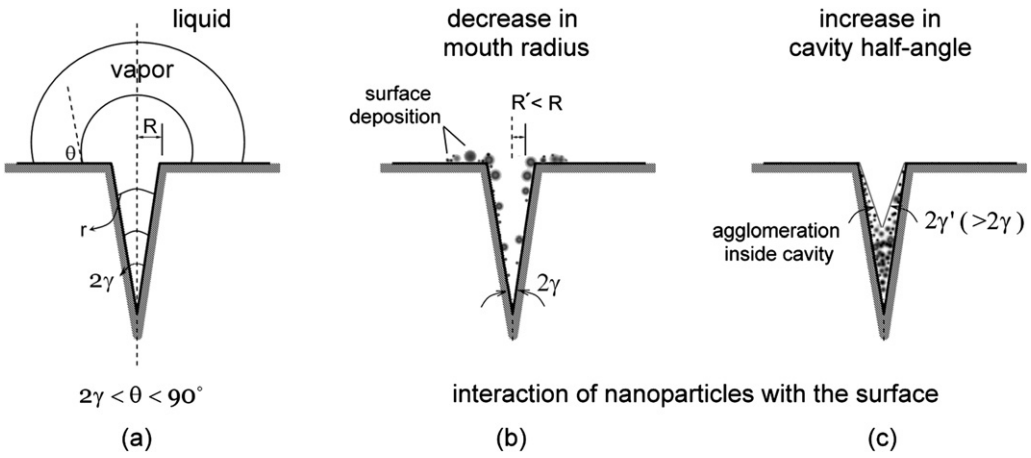

Fig. 4. A nucleating cavity (left) and possible physical adhesion/clogging of nanoparticles in the cavities thereby affecting mouth radius and cavity half-angle.

was prepared whose initial roughness was similar to that of inside surface of the thermosyphon container. The initial surface roughness of the substrate was found to be $R_a = 0.23$ μm, $R_z = 1.78$ μm and $R_q = 0.29$ μm. Two identical samples of the flat substrate were then separately boiled for two hours in the alumina and laponite nanofluids. Fig. 5 shows the surface morphology of the substrate, as viewed through an optical microscope (Zoom = 500 X) under different conditions. It is clearly seen that there is a considerable change in surface morphology of the sample after boiling in respective nanofluids. Agglomerates are clearly seen adhering to the surface of the substrate (the effect of these surface conditions on wettability is discussed later). The surface roughness of the sample after boiling in respective nanofluids was measured to be lower than the original substrate ($R_a = 0.20$ μm, $R_z = 1.66$ μm, $R_q = 0.25$ μm for alumina based nanofluid boiled substrate and $R_a = 0.18$ μm, $R_z = 1.62$ μm, $R_q = 0.24$ μm for laponite based nanofluid boiled substrate). Thus, it is quite evident that nanoparticles are getting entrapped in the nucleating surface cavities thereby reducing its size and degrading the active nucleation site density. These two modes, namely surface agglomeration and entrapment in cavities, are schematically depicted in Fig. 4(b, c). These mechanisms will slowly lead to cavity blockage and deactivation. Thus, deposition of nanoparticles due to sustained nucleation on the material surface is indeed degrading its surface quality for nucleation thereby reducing the heat transfer coefficient under nucleate boiling conditions.

In an evaporator section of the thermosyphon, following correlation between Nusselt number, Reynolds number and Prandtl number is generally considered to be valid [34]:

$$Nu = A \cdot Re^a \cdot Pr^b \tag{12}$$

Here, Nusselt number is hL_b/k_l (h is heat transfer coefficient in the evaporator section, L_b is length scale, generally chosen as the bubble departure diameter and k_l is liquid thermal conductivity), Reynolds number is $U_b L_b/v_l$ (U_b is velocity-scale of the bubble and v_l is the kinematic viscosity of the liquid) and Prandtl number corresponds to that of liquid. Since the concentration of nanoparticles in various nanofluids discussed

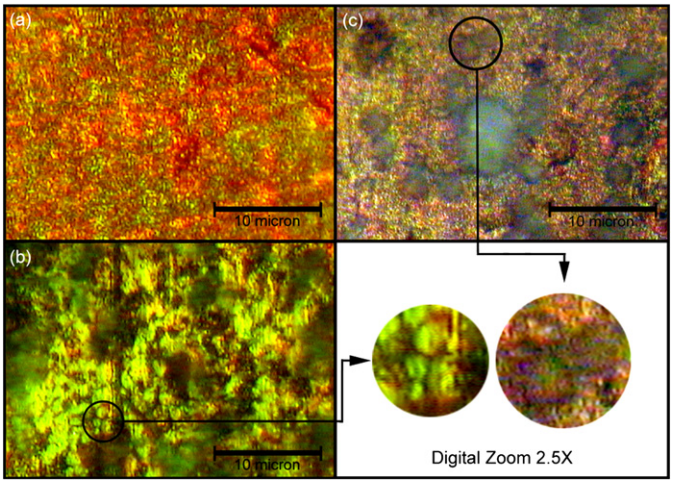

Fig. 5. Images from optical microscope showing: (a) virgin copper substrate, (b) copper substrate boiled in alumina nanofluid, (c) copper substrate boiled in laponite nanofluid. Inset shows digitally magnified images of agglomerated nanoparticles of alumina and laponite on copper substrate respectively.

in this paper is very small, it is justified to neglect any variation in Prandtl number due nanoparticles. Thus, we can assume that variation in evaporator side heat transfer occurs primarily due to change in effective Reynolds number pertaining to bubble movement. Furthermore, due to the same reason, change in kinematic viscosity can also be neglected upon addition of nanoparticles.[4] In literature, the effect of cavity (groove) half-angle and the contact angle between fluid and the solid substrate on the departing bubble size has been carefully analyzed [34].

[4] 1 weight % of the nanoparticle corresponds to a volume fraction of 0.005. In this limit, use of Einstein relationship [11] is justified which predicts an increase in viscosity by a factor of 1.0125. Also, increase in thermal conductivity of nanofluid cannot be expected to be more than 20% of that of the base fluid (water). Thus, change in effective Prandtl number will only be marginal. Furthermore, since we do not use any surfactants, surface tension does not have any additional effect on the heat transfer characteristics. This means that the mechanisms that tend to deteriorate the thermal performance are far more dominating than those that tend to enhance the same. Hence, to investigate all those degrading mechanisms, it is prudent to neglect marginal decrease in Prandtl number for the sake of scaling arguments, presented herein.

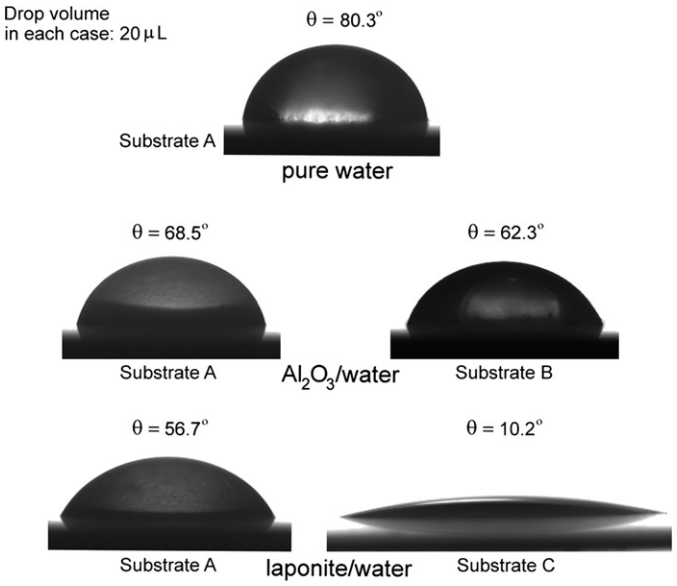

Fig. 6. Goniometer photographs of sessile droplets of different fluids. Substrate A: virgin copper substrate; Substrate B: copper substrate boiled in alumina nanofluid; Substrate C: copper substrate boiled in laponite.

As we have discussed earlier, nanofluid tends to increase the cavity half angle as compared to that of base fluid and its contact angle on the solid substrate also changes (more discussion later in the present section, refer to Fig. 6). In the limit of small variations of the cavity half angle and the contact angle, we can consider following relation to hold [34,35]:

$$L_b/R \sim \gamma^{-c}\theta^d \tag{13}$$

where c and d are positive constants. The velocity-scale of the departing bubble can be considered to be a product of frequency of the bubble departure and the bubble length scale (diameter). It is generally believed that frequency varies inversely with bubble diameter [34,35] and hence for the present argument, we can consider velocity-scale to be only weakly dependent on the cavity half angle and the contact angle. Thus, we can write:

$$Nu \sim \gamma^{-c}\theta^d \tag{14}$$

which shows that evaporator side heat transfer will be enhanced by decreasing the cavity half angle or by increasing the contact angle between fluid and the solid substrate. The thermal resistance defined in Eq. (7) is inversely proportional to evaporator side heat transfer coefficient. Larger the evaporator side heat transfer coefficient (or Nusselt number), smaller the thermal resistance is. Thus, it can be directly correlated that as the cavity (groove) half angle increase and/or as contact angle between fluid and the solid substrate decreases, the thermal resistance increases.

In Fig. 4 we postulate that, because of accumulation and/or trapping of nanoparticles in the cavity (or the groove), the cavity half-angle will tend to increase. Also, the average surface roughness, after continuous boiling, decreased due to entrapment of particle agglomerates inside the nucleating cavities. Furthermore, in order to investigate the effect of adding nanoparticles on surface wettability, static contact angles of sessile droplets of two nanofluids were measured on flat copper substrate (referred earlier for roughness tests) with the help of a goniometer. Fig. 6 shows the main results along with experimental conditions. The repeatability of the contact angle data was within ±5%. Two effects are clearly visible: (i) Even for the same substrate, there is a noticeable difference in the contact angle of nanofluids as compared to that of pure water. (ii) Sustained boiling of the nanofluid on the substrate changes its morphology thereby greatly affecting the wetting characteristics. In the present experiments, both the above effects results in substantial decrease in the contact angle. The fact that wettability of laponite clay based nanofluid was more pronounced than alumina based nanofluid also predicts its inferior thermal performance as observed experimentally.

Mixing of a nanoparticle in the liquid medium strongly affects its surface energy. In the background of the fact that van der Waals forces are effective within about 100 nm range, the length scales of the nanoparticles comes in the domain of influence of these forces [36]. Since the total surface free energy is the manifestation of interaction of different molecular forces (metallic bond, hydrogen bond, Keesom and Debye forces, London dispersion forces, covalent bonds etc.), their effect on bulk thermo-physical properties needs to be addressed while dealing with nanofluids. Although, the contact angle results of Fig. 6 are under static conditions, they clearly indicate the trends obtained in the thermal performance of the thermosyphon vis-à-vis Eq. (14). Also, given the fact that CHF improves with wettability, the trends regarding CFH mechanisms with nanofluids can be partly explained.

6. Summary and conclusions

A two-phase gravity assisted thermosyphon was designed, fabricated and tested with three nanofluids based on water (with 1% by weight of Al_2O_3, CuO, and laponite clay). Baseline thermal performance was obtained with pure water as the working fluid. In general, it is observed that thermal performance deteriorates when nanofluids are used as working fluids. Maximum deterioration was observed with laponite while minimum deterioration was for aluminum oxide particles based nanofluids.

Increased thermal conductivity of the nanofluids, as reported in the literature, does not appear to be affecting the nucleate pool boiling heat transfer coefficient (although single phase heat transfer improves, as suggested by literature). Boiling characteristics of nanofluids seems to be more affected by the physical interaction of nanoparticles with the nucleating cavities. It is likely that these particles agglomerate and/or accumulate due to vaporization and block the active cavities thereby reducing the active site density at a given wall superheat. Static contact angles of the used nanofluids on a copper substrate were measured and it was clearly seen that the nanofluids based on alumina and laponite have better wettability characteristics. Using simple scaling arguments, we show that improvement in wettability along with entrapment of nanoparticles in the grooves of surface roughness lead to deterioration of the thermal performance of nanofluid in closed two-phase thermosyphon. It also gives a clear suggestion to explain the trends that show improved CHF

values with nanofluids, which also gets affected by the wettability characteristics of the fluids.

Acknowledgements

The work is partially funded by IIT Kanpur, India (Faculty Initiation Grant #IITK/ME/20050019) and the Department of Mechanical Engineering. Help from Mr. Vivek Agnihotri and technical support from Mr. C.S. Goswami is appreciated.

References

[1] S.U.S. Choi, Enhancing thermal conductivity of fluids with nanoparticles, developments and applications of non-Newtonian flows, FED-vol. 231/MD-vol. 66, 1995, pp. 99–105.
[2] X. Wang, X. Xu, S.U.S. Choi, Thermal conductivity of nanoparticle–fluid mixture, J. Thermophys. Heat Transfer 13 (4) (1999) 474–480.
[3] P. Keblienski, S.R. Phillpot, S.U.S. Choi, J.A. Eastman, Mechanisms of heat flow in suspensions of nanosized particles (nanofluids), Int. J. Heat Mass Transfer 45 (2002) 855–863.
[4] J.A. Eastman, S.R. Phillpot, S.U.S. Choi, P. Keblinski, Thermal transport in nanofluids, Annu. Rev. Mater. Res. 34 (2004) 219–246.
[5] S.P. Jang, S.U.S. Choi, Role of Brownian motion in the enhanced thermal conductivity of nanofluids, Appl. Phys. Lett. 84 (2004) 4316–4318.
[6] S. Lee, S.U.S. Choi, S. Li, J.A. Eastman, Measuring thermal conductivity of fluids containing oxide nanoparticles, J. Heat Transfer 121 (1999) 280–289.
[7] Y. Xuan, Q. Li, Heat transfer enhancement of nanofluids, Int. J. Heat Fluid Transfer 21 (2000) 58–64.
[8] J.A. Eastman, S.U.S. Choi, S. Li, W. Yu, L.J. Thompson, Anomalously increased effective thermal conductivities of ethylene glycol-based nanofluids containing copper nanoparticles, Appl. Phys. Lett. 78 (6) (2001) 718–720.
[9] T.K. Hong, H.-S. Yang, C.J. Choi, Study of the enhanced thermal conductivity of Fe nanofluids, J. Appl. Phys. 97 (6) (2005) 1–4.
[10] S.K. Das, N. Putra, P. Thiesen, W. Roetzel, Temperature dependence of thermal conductivity enhancement for nanofluids, ASME Trans. J. Heat Transfer 125 (2003) 567–574.
[11] X. Wang, A.S. Mujumdar, Heat transfer characteristics of nanofluids: A review, Int. J. Thermal Sci. 46 (2007) 1–19.
[12] Y. Xuan, Q. Li, Investigation on convective heat transfer and flow features of nanofluids, J. Heat Transfer 125 (2003) 151–155.
[13] D. Wen, Y. Ding, Experimental investigation into convective heat transfer of nanofluids at the entrance region under laminar flow conditions, Int. J. Heat Mass Transfer 47 (24) (2004) 51–81.
[14] S. Heris, S.G. Etemad, M. Esfahany, Experimental investigation of oxide nanofluids under laminar flow convective heat transfer, Int. Comm. Heat Mass Transfer 33 (4) (2006) 529–535.
[15] B. Pak, Y. Cho, Hydrodynamic and heat transfer study of dispersed fluids with submicron metallic oxide particles, Exp. Heat Transfer 11 (2) (1998) 151–170.
[16] Y. Yang, Z.G. Zhang, E.A. Grulke, W.B. Anderson, G. Wu, Heat transfer properties of nanoparticle-in-fluid dispersions (nanofluids) in laminar flow, Int. J. Heat Mass Transfer 48 (6) (2005) 1107–1116.
[17] C.H. Li, B.X. Wang, X.F. Peng, Experimental investigations on boiling of nano-particle suspensions, in: 2003 Boiling Heat Transfer Conference, Jamaica, USA, 2003.
[18] S.K. Das, N. Putra, W. Roetzel, Pool boiling characteristics of nano-fluids, Int. J. Heat Mass Transfer 46 (5) (2003) 851–862.
[19] S.M. You, J.H. Kim, K.H. Kim, Effect of nanoparticles on critical heat flux of water in pool boiling heat transfer, Appl. Phys. Lett. 83 (2003) 3374–3376.
[20] I.C. Bang, Boiling heat transfer performance and phenomenon of Al_2O_3–water nanofluids from a plain surface in a pool, Int. J. Heat Mass Transfer 48 (2005) 2407–2419.
[21] J.P. Tu, N. Dinh, T. Theofanous, An experimental study of nanofluid boiling heat transfer, in: Proc. of 6th International Symposium on Heat Transfer, Beijing, China, 2004.
[22] P. Vassallo, R. Kumar, S. D'Amico, Pool boiling heat transfer experiments in silica–water nanofluids, Int. J. Heat Mass Transfer 47 (2004) 407–411.
[23] D. Milanova, R. Kumar, Role of Ions in pool boiling heat transfer of pure and silica nanofluids, Appl. Phys. Lett. 87 (233107) (2005).
[24] S.J. Kim, I.C. Bang, J. Buongiorno, L.W. Hu, Effects of nanoparticle deposition on surface wettability influencing boiling heat transfer in nanofluids, Appl. Phys. Lett. 89 (15) (2006).
[25] H. Kim, J. Kim, M. Kim, Experimental study on CHF characteristics of water–TiO_2 nanofluids, Nuclear Engrg. Technol. 38 (1) (2006).
[26] K. Sefiane, On the role of structural disjoining pressure and contact line pinning in critical heat flux enhancement during boiling of nanofluids, Appl. Phys. Lett. 89 (4) (2006).
[27] A. Faghri, Heat Pipe Science and Technology, Taylor and Francis, 1995.
[28] G.B. Wallis, One Dimensional Two-Phase Flow, McGraw–Hill Inc., 1969.
[29] A. Faghri, M.M. Chen, M. Morgan, Heat transfer characteristics in two–phase closed conventional and concentric annular thermosyphons, Trans. ASME J. Heat Transfer 111 (1989) 611–618.
[30] C.L. Tien, K.S. Chung, Entrainment limits in heat pipes, in: Proc. 3rd Int. Heat Pipe Conf., Palo Alto, AIAA, 1978, pp. 36–40.
[31] I. Golobič, B. Gašperšič, Corresponding states correlation for maximum heat flux in two-phase closed thermosyphon, Int. J. Refrigeration 20 (6) (1997) 402–410.
[32] H. Imura, K. Sasaguchi, H. Kozai, S. Numata, Critical heat flux in two phase closed thermosyphon, Int. J. Heat Mass Transfer 26 (8) (1983) 1181–1188.
[33] S.S. Kutateladze, Elements of hydrodynamics of gas–liquid systems, Fluid Mech.-Sov. Res. 1 (1972) 29–50.
[34] P. van Carey, Liquid Vapor Phase Change Phenomena, second ed., ISBN 1591690358, Taylor and Francis, 2007.
[35] C. Stephan, Heat Transfer in Condensation and Boiling, in: A.E. Bergles, F. Mayinger (Eds.), International Series in Heat and Mass Transfer, ISBN 0387-52203-4, Springer-Verlag, 1992.
[36] J.N. Israelachvili, Intermolecular and Surface Forces, 10th reprint, ISBN 0-12-375181-0, Academic Press, 2003.